A Common Method of Share Authentication in Image Secret Sharing

Xuehu Yan, Yuliang Lu, Ching-Nung Yang, *Senior Member, IEEE*, Xinpeng Zhang, and Shudong Wang

***Abstract*— Because of the importance of digital images and their extensive application to digital watermarking, block chain, access control, identity authentication, distributive storage in the cloud and so on, image secret sharing (ISS) is attracting ever-increasing attention. Share authentication is an important issue in its practical application. However, most ISS schemes with share authentication ability require a dealer to participate in the authentication (namely, dealer participatory authentication). In this paper, we design an ISS for a (k, n)-threshold with separate share authentication abilities of both dealer participatory authentication and dealer nonparticipatory authentication. The advantages of polynomial-based ISS and visual secret sharing (VSS) are skillfully fused to achieve these two authentication abilities without sending a share by using a screening operation. In addition, the designed scheme has the characteristics of low decryption (authentication) complexity, lossless decryption and no pixel expansion. Experiments and theoretical analyses are performed to show the effectiveness of the designed scheme.**

***Index Terms*— Image secret sharing, lossless recovery, share authentication, no pixel expansion.**

I. Introduction

IN PACE with the extensive development and application of multimedia technology, digital multimedia data are easily gained, conveyed and managed. Therefore, the security of digital multimedia is crucial for protecting susceptible multimedia data from malicious interference in the process of public channel transmission. To guarantee the security of multimedia, cryptography and information hiding are considered. By encryption and decryption operations using secret keys [1], cryptographic techniques transform the multimedia data between incomprehensible and comprehensible forms. Information hiding [2], [3] embeds multimedia data into digital cover media. However, for several reasons, the cover media's data are unavoidably destroyed or lost. As a result, the embedded multimedia data will be unavailable. To overcome this restriction, secret sharing has been put forward.

In the generation period, a (k, n) threshold secret sharing scheme divides the multimedia data into n shares, named shadow images or shadows. According to the scheme, those images are assigned to the corresponding n participants; in the recovery period, the multimedia data are recovered when k or more shares are obtained. Furthermore, regardless of how computationally powerful the device an attacker has, he cannot obtain any information about the multimedia data. As a result, secret sharing can potentially be applied to some scenarios [4], such as block chain [5], key management [6], digital watermarking [7], [8], identity authentication [9], [10], and distributive storage [11], [12].

As one of the most important media types, a digital image carries considerable information. Hence, image secret sharing (ISS) has been widely studied. ISS encrypts a digital secret image into some shares, *a.k.a.*, shadow images or shadows, and then assigns them to the corresponding participants. Losing at most $n-k$ shares, the dealer can decrypt the secret image as well. Moreover, it is called a loss-tolerant feature in (k, n)-threshold ISS. The encrypting principles of traditional ISS technologies are mainly comprised of visual secret sharing (VSS) [13]–[15], namely, visual cryptography (VC), polynomials [16], etc., [17]–[19], where polynomial-based ISS and VSS are also the chief research branches of ISS.

In a (k, n)-threshold VSS [20]–[22], the output n shares are first printed onto transparencies and subsequently distributed to n participants. No computational device is required to decrypt the secret image from greater than or equal to k shares. Superpose them, and they can be recognized with only the naked human eye. If an attacker steals less than $k-1$ shares, regardless of how computationally powerful the device he uses, he cannot decrypt the secret image as well. However, there are also some shortcomings in the traditional VSS schemes, such as poor image quality and pixel expansion, which have been further studied in the follow-up studies [23]–[25] especially random grid-based VSS (RG-VSS).

Shamir [16] first exploited a polynomial-based secret sharing algorithm for (k, n)-threshold to decrypt a secret image with high quality, in which the dealer generates the output n shares through constructing a $(k-1)$-degree polynomial. Then, the shares are sent to corresponding participants by the dealer, as shown in Fig. 1. In the normal decrypting

Manuscript received September 2, 2020; accepted September 15, 2020. Date of publication September 21, 2020; date of current version July 2, 2021. This work was supported in part by the Key Program of the National University of Defense Technology under Grant ZK-17-02-07 and in part by the National Natural Science Foundation of China under Grant 61602491. This article was recommended by Associate Editor X. Cao. *(Corresponding author: Xuehu Yan.)*

Xuehu Yan, Yuliang Lu, and Shudong Wang are with the College of Electronic Engineering, National University of Defense Technology, Hefei 230037, China (e-mail: ictyanxuehu@163.com; publicLuYL@126.com; shudong0905@163.com).

Ching-Nung Yang is with the Department of Computer Science and Information Engineering, National Dong Hwa University, Hualien 974, Taiwan (e-mail: cnyang@gms.ndhu.edu.tw).

Xinpeng Zhang is with the School of Computer Science, Fudan University, Shanghai 200433, China (e-mail: zhangxinpeng@fudan.edu.cn).

Color versions of one or more of the figures in this article are available online at https://ieeexplore.ieee.org.

Digital Object Identifier 10.1109/TCSVT.2020.3025527

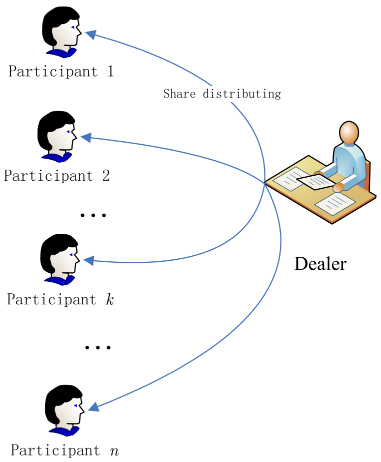

Fig. 1. The share distributing phase in image secret sharing.

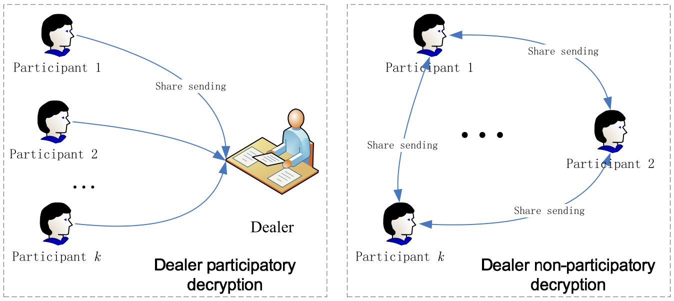

Fig. 2. The normal secret decryption in image secret sharing.

phase, there are two choices, as shown in Fig. 2, *a.k.a.*, dealer participatory decryption and dealer nonparticipatory decryption. **For the dealer participatory decryption**, when any k or more participants send their shares to the dealer, the dealer decrypts the secret with good quality by Lagrange interpolation. **For the dealer nonparticipatory decryption**, when a participant exchanges the share with any other $k-1$ participants, the participant decrypts the secret with good quality by Lagrange interpolation. After Shamir's work, many works [26]–[29] developed improved polynomial-based ISS schemes to obtain desirable properties. Polynomial-based ISS is significant because the decrypted secret image has no pixel expansion and high quality. However, ISS has shortcomings in that the decrypted secret image is in general a slightly distorted or auxiliary encryption is utilized to avoid secret information leakage.

More importantly, the abovementioned ISS schemes have not considered the share authentication ability. Share authentication plays an important role in practical application of ISS, as shown in Fig. 3. In an abnormal secret image decryption without authentication, **for the dealer participatory decryption**, after any k or more shares are collected, if there exists a fake participant among the k participants in an abnormal decrypting phase without authentication, the dealer fails to decrypt the secret image and cannot even distinguish the fake one; **for the dealer nonparticipatory decryption**, the current participant fails to decrypt the secret image and does not distinguish the fake one. More importantly, her real share is already sent to the fake participant.

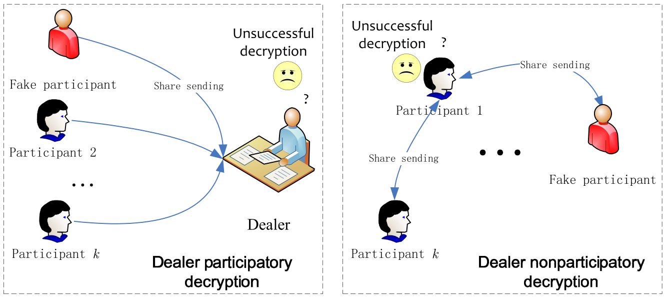

Fig. 3. The abnormal secret decryption in image secret sharing without authentication.

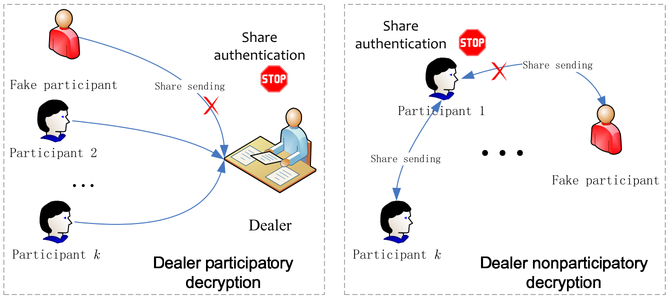

Fig. 4. The abnormal secret decryption in image secret sharing with authentication.

However, in an abnormal secret image decryption phase with authentication, as shown in Fig. 4, **for the dealer participatory decryption**, the dealer judges whether the share is fake or not based on the result of share authentication when receiving each share from any participant, stops the decryption phase if a fake share is identified, and broadcasts the fake participant to the others; **for the dealer nonparticipatory decryption**, in a similar way, the current participant authenticates the possible exchanged share prior to sending her real share.

Share authentication is an important issue in practical applications, and it is significant for ISS. Therefore, ISS with share authentication ability is attracting more attention. It is easy to develop ISS with share authentication by information hiding (such as, fragile watermark) [30]–[32] and hash functions [33], [34]. One representative work is that of [31], where Liu and Chang achieve share authentication, and the key idea is derived from a turtle shell-based information hiding. As a result, most ISS schemes with share authentication ability embed the shares into cover images by existing information hiding techniques; however, this approach leads to high encryption and decryption (authentication) complexity and a possible pixel expansion.

Liu *et al.* [35] extended polynomial-based ISS for (k, n) threshold with share authentication by using improved polynomial-based ISS, in which the authenticating value is embedded into a selected coefficient of the polynomial. Unfortunately, it suffers from lossy decryption, hard fake participant location, high encryption and decryption (authentication) complexity, and auxiliary encryption. Recently, Yan *et al.* [36] proposed a (k, n) threshold ISS scheme with a separate share authentication by applying (2,2) threshold VSS to polynomial-based ISS. In the generating process, the most significant bit (MSB) of each share pixel is equal to one share bit in VSS. Their scheme can achieve lossless recovery with no auxiliary encryption. However, it has the limitations of only dealer participatory authentication and information leakage with larger values of $n - k$. Inspired by Yan *et al.*'s work, Jiang *et al.* [37] further developed a scheme suitable for dealer nonparticipatory authentication by applying $(2, n + 1)$ threshold VSS and setting the least significant bit (LSB) of every share pixel equal to one share bit in VSS. Unfortunately, it needs a larger encrypting time and authentication may fail with a larger value of $n - k$.

Under the conditions of no pixel expansion, no auxiliary encryption and separate share authentication, achieving ISS and based on ISS itself suitable for both dealer participatory authentication and dealer nonparticipatory authentication is a key challenge.

The motivation of this paper is to design an ISS for the (k, n)-threshold with separate common share authentication ability, where "common" means the authentication is suitable for both dealer participatory authentication and dealer nonparticipatory authentication. Here, dealer participatory authentication means that the dealer needs to participate in the authentication to achieve share authentication; dealer nonparticipatory authentication means that the dealer does not need to participate in the authentication to achieve share authentication. Since the designed ISS is suitable for both dealer participatory authentication and dealer nonparticipatory authentication, it has a wider range of application scenarios.

In the scheme, a sharing grayscale secret image and a binary authentication image are input to output n grayscale shares with $P = 257$. Here, P is a prime number and all the computations will be performed in the prime field. Polynomial-based ISS can decrypt a secret image with high quality. The decryption of VSS is simple and role-independent. The advantages of VSS and polynomial-based ISS are skillfully fused to achieve these two authentication abilities without sending shares by using a screening operation. Here, a "screening operation" is an operation that screens the polynomial coefficients satisfying some requirements. We actually use a screening operation to fuse VSS and polynomial-based ISS.

In the process of encrypting each secret image pixel, by using a screening operation on some random coefficients of a constructed polynomial, the XORing result of the four low bits of the value of each share pixel is equal to one temporary encrypting bit from the binary authentication image by the $(2, n + 1)$ threshold VSS, and the value of each share pixel is less than 256. In the authentication and decryption phase, the participant is authenticated by only XORing and stacking operations with two choices, *a.k.a.*, dealer participatory and dealer nonparticipatory. Since the decryption of VSS is role-independent, the proposed scheme is a common scheme for dealer participatory and dealer nonparticipatory scenarios. By passing the share authentication, the secret image will be losslessly decrypted by Lagrange interpolation with any k or more shares. In addition, the designed scheme has the characteristics of low decryption (authentication) complexity, lossless decryption, no pixel expansion and no auxiliary encryption. Experiments and theoretical analyses are performed to verify the effectiveness.

The following sections are presented in the following way. Section II introduces some preliminaries for our work. In section III, we show the designed common method of share authentication in ISS and its performance analyses. Section IV demonstrates the experiments and comparisons, and finally section V concludes this paper.

II. Preliminaries

In this section, some preliminary work is illustrated, including image feature analysis, RG-VSS for the $(2, 2)$ threshold and original polynomial-based ISS schemes. To achieve lossless decryption and avoid auxiliary encryption in the designed scheme, the feature of an image is analyzed; RG-VSS for the $(2, 2)$ threshold is used to encrypt each binary authentication pixel into two random bits; traditional polynomial-based ISS schemes are the foundation of our scheme. By using a screening operation, our scheme realizes the independent public sharing authentication ability. In conventional ISS for the (k, n) threshold, a secret image S_2 is encrypted into n shares $SC_1, SC_2, \cdots SC_n$, and the decrypted secret image $S_2{}'$ is decrypted from t $(k \leq t \leq n, t \in \mathrm{Z}^+)$ shares.

A. The Feature Analyses of a Digital Image

A digital image is a specific data format, but there are some specific features about it that should be taken into account when designing an ISS scheme.

1) The value of each pixel in an image is associated with its adjoining ones to form texture, structure, edges and so on. In particular, in a local region of an image, the grayscale value of one pixel resembles its adjoining pixels.
2) An image includes generous pixels with a large amount of data; therefore, the efficiency is of sovereign significance.
3) An image has its specific coding method to store the image file. In particular, for a grayscale image, its pixel values range from 0 to 255. Thus, the value of each output share pixel and the value of the input secret pixel should also range from 0 to 255.
4) Using one byte represents the value of each grayscale pixel, an ISS technique is easily extended to an SS technique. The value of one binary pixel is represented by one bit, and the value of one grayscale pixel is represented by one byte. An ISS technique can process an image absolutely including each grayscale pixel, e.g., one byte; ordinary data is composed of byte. This is why we say that ISS technique can be easily extended to SS technique. In general, VSS is applied to key management covered by a binary image. It is not be suitable for data security, simply because ordinary data are not visual data. However, in some special cases, VSS may be

suitable for data security, such as XOR-based VSS. XOR-based VSS with the feature of lossless recovery may process ordinary data because XOR-based VSS can process one binary pixel represented by one bit. Of course, whether XOR-based VSS belongs to the field of classic VSS is another issue.

B. Random Grid-Based VSS (RG-VSS)

RG-VSS is close to probabilistic VSS [38], [39]. The RG encryption procedure in RG-VSS replaces the codebook (basic matrix) design in probabilistic VSS. Thus, in this paper, only RG-VSS is used as an example.

In RG-VSS [24], [40], '0' denotes a white pixel and '1' denotes a black pixel. The encrypting and decrypting phases of a typical $(2, 2)$ RG-VSS are presented as follows.

Encrypting Step 1: Using a coin flipping function to encrypt 1 RG S_1C_1 pseudorandomly.

Encrypting Step 2: Using Eq. (1) to calculate S_1C_2.

Decrypting phase: $S_1{}' = S_1C_1 \otimes S_1C_2$ as Eq. (2), where $\otimes$ indicates stacking (Boolean OR) decryption.

$$S_1C_2(h,w) = \begin{cases} S_1C_1(h,w) & if\ S_1(h,w) = 0 \\ \overline{S_1C_1(h,w)} & if\ S_1(h,w) = 1 \end{cases} \tag{1}$$

$$\begin{aligned} S_1'(h,w) &= S_1C_1(h,w) \otimes S_1C_2(h,w) \\ &= \begin{cases} S_1C_1(h,w) \otimes S_1C_1(h,w) & if\ S_1(h,w) = 0 \\ S_1C_1(h,w) \otimes \overline{S_1C_1(h,w)} = 1 & if\ S_1(h,w) = 1 \end{cases} \end{aligned} \tag{2}$$

$AS0$ (resp., $AS1$) is a white (resp., black) area of S_1, *a.k.a.*, $AS0 = \{(h,w) | S_1(h,w) = 0, 1 \le h \le H, 1 \le w \le W\}$ (resp., $AS1 = \{(h,w) | S_1(h,w) = 1, 1 \le h \le H, 1 \le w \le W\}$).

For any pixel s_1 of S_1, the probability that the pixel color is white or transparent (0) is represented by $P(s = 0)$, and the probability that the pixel color is black or opaque (1) is represented by $P(s = 1)$. $P(S = 0) = 1 - P(S = 1) = 1 - \frac{1}{HW} \sum_{i=1}^{H} \sum_{j=1}^{W} S(h,w), 1 \le h \le H, 1 \le w \le W$.

Definition 1 (Contrast): The image quality of the decrypting secret image $S_1{}'$ in VSS is in general evaluated by contrast, denoted by α, as follows [24]:

$$\alpha = \frac{P_0 - P_1}{1 + P_1} = \frac{P(S_1{}'[AS0] = 0) - P(S_1{}'[AS1] = 0)}{1 + P(S_1{}'[AS1] = 0)} \tag{3}$$

In which P_1 denotes the error decrypting probability of the black area of S_1 and P_0 denotes the correct decrypting probability of the white area of S_1.

The contrast will to some degree determine how well human eyes may recognize the decrypted binary secret image. For clarity corresponding to different contrast values, please refer to [41].

C. Polynomial-Based ISS Scheme

To encrypt a grayscale secret image, denoted by S_2, the primitive of Shamir's polynomial-based ISS method is used to encrypt the secret pixel value s_2 into n corresponding pixels distributed to corresponding n shares. The designed scheme uses part of the thought of the primitive of Shamir's polynomial-based ISS scheme. The primitive scheme is presented below.

```
Algorithm Shamir's Polynomial-Based ISS
  Input: A grayscale secret image $S_2$ with size of $H \times W$, and the threshold parameters $(k, n)$
  Output: $n$ shares $S_2C_1, S_2C_2, \cdots S_2C_n$

  Step 1: $P = 251$ is selected. For each position $(h, w) \in \{(h, w) | 1 \le h \le H, 1 \le w \le W\}$, repeat Steps 2-4
  Step 2: For $s_2 = S_2(h, w)$, if $s_2 \ge P$, set $s_2 = P - 1$. To encrypt $s_2$ into pieces $s_2c_1, s_2c_2, \cdots s_2c_n$, a $k - 1$ degree polynomial is constructed as follows.
      $f(x) = (a_0 + a_1x + \cdots + a_{k-1}x^{k-1}) \bmod P$    (4)
    in which $a_0 = s_2$, and $a_i$ is random, for $i = 1, 2, \cdots k - 1$.
  Step 3:
      $s_2c_1 = f(1), \cdots, s_2c_i = f(i), \cdots, s_2c_n = f(n)$.    (5)
    where $i$ is in general served as an order label or an identifying index for the $i$-th participant.
  Step 4: Assign $s_2c_1, s_2c_2, \cdots s_2c_n$ to $S_2C_1(h,w)$, $S_2C_2(h,w)$, $\cdots S_2C_n(h, w)$.
  Step 5: Output the $n$ shares $S_2C_1, S_2C_2, \cdots S_2C_n$.
```

In the decrypting phase, as long as given any k pairs of the n pairs $\{(i, s_2c_i)\}_{i=1}^{n}$, the coefficients of $f(i)$ can be solved by Lagrange interpolation and then set $s_2 = f(0)$. With any less than k shares, the secret s_2 cannot be universally solved.

III. The Designed ISS With Separate Common Share Authentication Ability

A. The Designed Scheme

The idea of the designed ISS for the (k, n)-threshold with separate share authentication abilities of both dealer participatory authentication and dealer nonparticipatory authentication, denoted by ISSCommonAuthen for short, is illustrated in Fig. 5. The detailed encrypting algorithm is in **Algorithm 1**, and its corresponding decrypting method is in **Algorithm 2**.

Regarding Algorithm 1, we note the following.

1) A binary authentication image S_1 is input by the dealer and known among all the participants. The dealer can replace it by setting an authentication password converted into a binary image such as "HIT" as well, which refrains from storing an image.
2) Selecting the prime number $P = 257$ in step 1, the sharing pixel in the range of$[0, 255]$and lossless decryption is realized by using screening operation in Step 4 $S_2C_i\ (h, w) < P - 1$.
3) The purpose of Step 3 is to use the polynomial to realize the characteristics of no pixel expansion and the (k, n) threshold.
4) Step 4 is designed to meet the requirements of $XOR4LBs\ (S_2C_i\ (h, w)) = S_1C_i\ (h, w)$ to realize share authentication with only $XOR4LBs\ (S_2C_i\ (h, w))$.

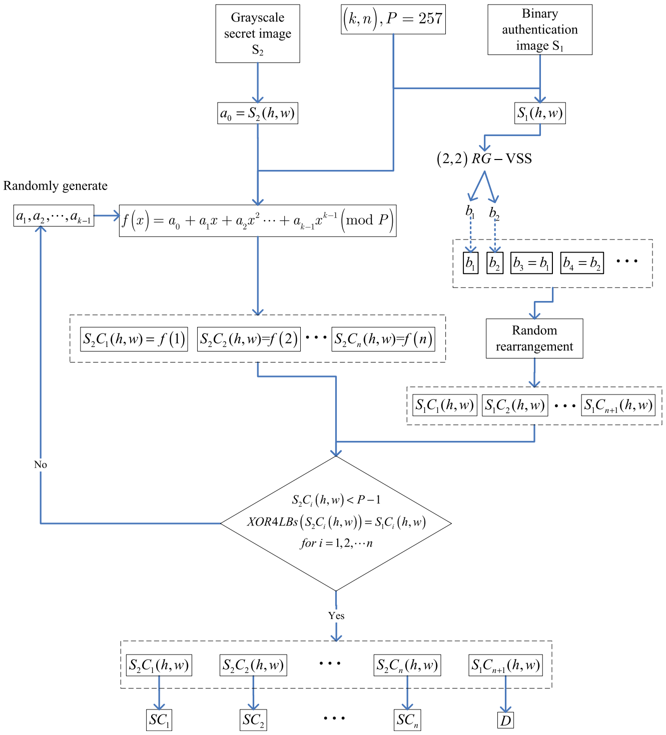

Fig. 5. Design idea of the designed image secret sharing with common share authentication ability.

5) The performance is enhanced by utilizing the randomness of $b_1, b_2, \cdots b_{n+1}$.
6) Because grayscale $a_1, a_2, \cdots, a_{k-1}$ are random, when $n-k$ is small we screen the random values in order to satisfy $S_2C_i\,(h, w) < P-1$ and $XOR4LBs\,(S_2C_i\,(h, w)) = S_1C_i\,(h, w)$, for $i = 1, 2, \cdots n$ in Step 4. In this way, S_2 can be losslessly decrypted and common share authentication ability is realized.

Regarding Algorithm 2, we note the following.

1) Before sending the corresponding share, the $XOR4LBs(SC_{i_j})$ can be easily obtained.
2) In Step 1 for case 1, the dealer collects shares to check whether S_1' is recognized as S_1 by HVS to complete authentication. Thus, our method based on XORing and stacking operations could realize separate share authentication for the dealer participatory case; for case 2, each received $XOR4LBs(SC_{i_q})$ is authenticated by the participant to check whether S_1' is recognized as S_1 by HVS. Thus, our method based on XORing and stacking operations realizes any two shares' authentication ability by two participants themselves for the case of dealer nonparticipatory authentication.

B. Security Analysis and Proof

Here, we show the security analysis and performance proof of the designed ISSCommonAuthen.

In the following, we assume that both the authentication image S_1 and the grayscale secret image S_2 are natural images, which are independent on each other, namely, they have no correlation.

Algorithm 1 The Designed Image Secret Sharing With Common Share Authentication Ability (ISSCommonAuthen)

```
Input: A binary authentication image $S_1$ with a size of $H \times W$; a grayscale secret image $S_2$ with a size of $H \times W$; threshold parameters $(k, n)$, where $2 \le k \le n$.
Output: Share $SC_i$, $i = 1, 2, \cdots n$, and a binary authentication share $D$.
Step 1: Select $P = 257$. For $(h, w) \in \{(h, w)|1 \le h \le H, 1 \le w \le W\}$ , repeat Steps 2-5.
Step 2: Employ $(2, 2)$ RG-VSS to encrypt $S_1(h, w)$ to two temporary bits, denoted by $b_1$ and $b_2$.
    Compute $b_3 = b_1, b_4 = b_2, \cdots$ if $(n+1 \mod 2) = 0, b_{n+1} = b_2$ else $b_{n+1} = b_1$.
    Rearrange randomly $b_1, b_2, \cdots b_{n+1}$ to $S_1C_1(h, w), S_1C_2(h, w), \cdots S_1C_{n+1}(h, w)$.
Step 3: Construct a following $k-1$ degree polynomial.
    $f(x) = (a_0 + a_1x + \cdots + a_{k-1}x^{k-1}) \bmod P$    (6)
    where $a_0 = S_2(h, w)$, and $a_i$ is random, for $i = 1, 2, \cdots k-1$.
    Compute $S_2C_i\,(h, w) = f(i)$, for $i = 1, 2, \cdots n$.
Step 4: Let $XOR4LBs(a)$ represent the XORing result of the four lower bits of $a$. If $S_2C_i\,(h, w) < P-1$ and $XOR4LBs\,(S_2C_i\,(h, w)) = S_1C_i\,(h, w)$, for $i = 1, 2, \cdots n$, go to Step 5; otherwise, go to Step 3.
Step 5: Assign $S_2C_i\,(h, w)$ to $SC_i\,(h, w)$, for $i = 1, 2, \cdots n$.
    Set $D(h, w) = S_1C_{n+1}(h, w)$.
Step 6: Output the $n$ grayscale shares $SC_1, SC_2, \cdots SC_n$, and a binary authentication share $D$ for the dealer.
```

We assume that the collected k grayscale pixels are denoted by $sc_{i_1}, sc_{i_2}, \cdots sc_{i_k}$ in the decryption phase corresponding to $SC_{i_1}(h, w), SC_{i_2}(h, w), \cdots SC_{i_k}(h, w)$. s_2 and s_1 mean $S_2(h, w)$ and $S_1(h, w)$, respectively.

Lemma 1: s_2 and sc_i can range from 0 to 255 for $i = 1, 2, \cdots n$.

Proof: Due to $P = 257$, s_2 can range from 0 to 255. $S_2C_i\,(h, w) < P-1$, sc_i can range from 0 to 255 for $i = 1, 2, \cdots n$. □

Theorem 1: Stacking any two of $S_1C_1, S_1C_2, \cdots S_1C_{n+1}$, the binary secret image S_1 is decrypted with contrast

$$\alpha = \begin{cases} \dfrac{\frac{1}{2} - \dfrac{C^2_{\frac{n+1}{2}}}{C^2_{n+1}}}{1 + \dfrac{C^2_{\frac{n+1}{2}}}{C^2_{n+1}}} & when\ n+1\ is\ even \\[2ex] \dfrac{\frac{1}{2}\left(1 - \dfrac{C^2_{\frac{n}{2}} + C^2_{\frac{n+2}{2}}}{C^2_{n+1}}\right)}{1 + \frac{1}{2}\dfrac{C^2_{\frac{n}{2}} + C^2_{\frac{n+2}{2}}}{C^2_{n+1}}} & when\ n+1\ is\ odd. \end{cases}$$

Proof: According to Eqs. (1) and (2), if the value of a secret pixel s_1 is 1 (black), the decrypted bit $b_1 \otimes b_2 = 1$ is always black; If the value of a secret pixel is 0, the decrypted

Algorithm 2 The Decryption and Authentication in the Designed Image Secret Sharing With Common Share Authentication Ability

```
Input: Any $k$ grayscale shares $SC_{i_1}, SC_{i_2}, \cdots SC_{i_k}$, a binary authentication share $D$ and a binary authentication image $S_1$.
Output: Decrypted grayscale secret image $S'_2$ with a size of $H \times W$ and authenticating result of $SC_{i_j}$, for $j = 1, 2, \cdots, k$.
Step 1: The authentication can be divided into two cases.
Case 1: dealer participatory authentication. For $j = 1, 2, \cdots, k$, compute $XOR4LBs(SC_{i_j})$, and stack $XOR4LBs(SC_{i_j})$ and $D$ to obtain the decrypted binary authentication image $S'_1$. If $S'_1$ is recognized as $S_1$ by HVS, pass the authentication and go to Step 2; otherwise, a fake share is identified, denoted by $i^*_j$, and immediately broadcast the fake one to the other participants.
Case 2: dealer nonparticipatory authentication. For the $i_p$-th participant, prior to share $SC_{i_p}$ with the $i_q$-th participant for $q = \{1, 2, \cdots, k\} \backslash p$, send $XOR4LBs(SC_{i_p})$ and $XOR4LBs(SC_{i_q})$ to each other first, and stack $XOR4LBs(SC_{i_p})$ and $XOR4LBs(SC_{i_q})$ to obtain the decrypted binary authentication image $S'_1$. Here, $q$ means any one of $\{1, 2, \cdots, k\}$ except $p$. If $S'_1$ is recognized as $S_1$ by HVS, pass the authentication, send their shares to each other and go to Step 2; otherwise, a fake share is identified, denoted by $i^*_j$, and immediately broadcast the fake one to the other participants with $S_1$ and $XOR4LBs(SC_{i_p})$.
Step 2: For each position $(h, w) \in \{(h, w) | 1 \leq h \leq H, 1 \leq w \leq W\}$, repeat Steps 3-4.
Step 3: Solve Eq. (7) to obtain $a_0$ by Lagrange interpolation.
    $f(i_1) = (a_0 + ai_1 + \cdots + a_{k-1}{i_1}^{k-1}) \bmod P$
    $f(i_2) = (a_0 + ai_2 + \cdots + a_{k-1}{i_2}^{k-1}) \bmod P$
    $\cdots$
    $f(i_{k-1}) = (a_0 + ai_{k-1} + \cdots + a_{k-1}{i_{k-1}}^{k-1}) \bmod P$
    $f(i_k) = (a_0 + ai_k + \cdots + a_{k-1}{i_k}^{k-1}) \bmod P$    (7)
Step 4: Compute $S'_2(h, w) = a_0$.
Step 5: Decrypted grayscale secret image $S'_2$ with a size of $H \times W$ and authenticating result of $SC_{i_j}$ for $j = 1, 2, \cdots, k$.
```

bit $b_1 \otimes b_2$ has a 0.5 chance to be white or black since b_1 is random.

In Step 2 of **Algorithm 1**, we have $b_3 = b_1, b_4 = b_2, \cdots$. When stacking any two bits of $b_1, b_2, \cdots, b_{n+1}$, if the value of a secret pixel is 0, we have $P_0 = \frac{1}{2}$; if the value of a secret pixel s_1 is 1 (black), we assume that $C_x^2 = 0$ when $x < 2$, we have

$$P_1 = \begin{cases} \dfrac{C^2_{\frac{n+1}{2}}}{C^2_{n+1}} & when\ n+1\ is\ even \\ \dfrac{1}{2} \dfrac{C^2_{\frac{n}{2}} + C^2_{\frac{n+2}{2}}}{C^2_{n+1}} & when\ n+1\ is\ odd \end{cases}$$

Finally, based on definition 1, the theorem is satisfied. □

Theorem 2: Using S_1 and any two of D and $SC_1, SC_2, \cdots SC_n$, we will authenticate whether SC_i is fake, for $i = 1, 2, \cdots n$.

Proof: In Step 4 of **Algorithm 1**, $XOR4LBs\,(S_2C_i\,(h, w)) = S_1C_i\,(h, w)$, for $i = 1, 2, \cdots n$.

According to theorem 1, stacking any two of D and $SC_1, SC_2, \cdots SC_n$, the binary secret image S_1 is visually decrypted. As a result, using S_1 and any two of D and $SC_1, SC_2, \cdots SC_n$, we will authenticate whether SC_i is fake, for $i = 1, 2, \cdots n$. □

Theorem 3: Our designed scheme is a valid ISS approach for the (k, n) threshold with lossless decryption when $n - k$ is limited.

Proof: From Lagrange interpolation and Eq. (7), we can determine a_0 and a_i uniquely for $i = 1, 2, \cdots k-1$. According to Lemma 1, $s_2 = a_0 < P$; hence, s_2 can be losslessly decrypted with $sc_{i_1}, sc_{i_2}, \cdots sc_{i_k}$.

If in Eq. (7) only $k - 1$ equations are constructed, we have P solutions rather than a unique one to Eq. (7). As a result, the secret image S_2 cannot be decrypted with $k - 1$ or fewer shares.

According to the definition of a (k, n)-threshold, the mentioned conditions are satisfied.

In general, grayscale $a_1, a_2, \cdots, a_{k-1}$ are random; thus, the number of possible random values are 256^{k-1}. To satisfy $S_2C_i\,(h, w) < P - 1$ and $XOR4LBs\,(S_2C_i\,(h, w)) = S_1C_i\,(h, w)$, for $i = 1, 2, \cdots n$, N_A will decrease to $256^{k-1} \times \left(\frac{256}{257} \times \frac{1}{2}\right)^n = \left(\frac{1}{2}\right)^n \times \frac{256^{n+k-1}}{257^n}$, where N_A indicates the number of available random values of $a_1, a_2, \cdots, a_{k-1}$ satisfying $S_2C_i\,(h, w) < P - 1$ and $XOR4LBs\,(S_2C_i\,(h, w)) = S_1C_i\,(h, w)$, for $i = 1, 2, \cdots n$.

N_A is related to security and encrypting efficiency. A larger N_A will result in higher encrypting efficiency and security because the number of brute-force attacks will be higher. We require $N_A \geq 2$ since if $N_A = 1$, a unique random value is repeatedly used, which is not secure. $N_A \geq 4$ is suggested for an acceptable performance. Moreover, $\frac{n-k}{n} \leq \frac{1}{2}$ is suggested for an acceptable performance. □

IV. Experimental Results

In this section, experiments are performed to verify the effectiveness of the designed ISSCommonAuthen. Then, parameters will be discussed. Finally, feature comparisons with related schemes are performed to clarify the advantages of our scheme. We assume that there is no noise in each share because we mainly focus on share authentication rather than robustness.

A. Image Illustration

In the experiments, since there is no pixel expansion in the designed ISS, the illustrated test images have the same size of 256 × 256.

Fig. 6 displays the results of the designed ISSCommonAuthen, where $k = 2, n = 2$, a binary authentication image S_1 is demonstrated in Fig. 6 (a) and a grayscale secret image S_2 is presented in Fig. 6 (b). Figs. 6 (c-d) indicate the output of 2 grayscale shares SC_1 and SC_2. Fig. 6 (e) shows the output

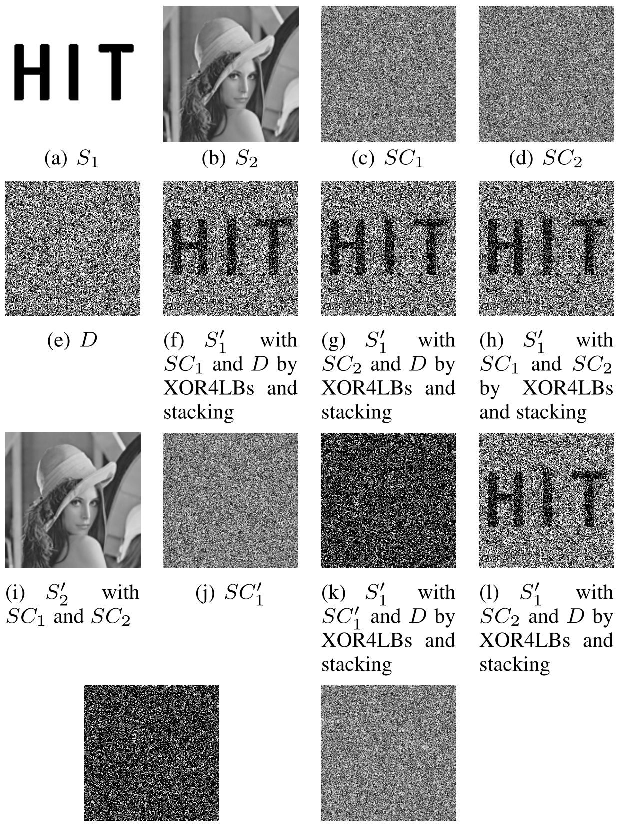

(a) S_1 (b) S_2 (c) SC_1 (d) SC_2

(e) D (f) S_1' with SC_1 and D by XOR4LBs and stacking (g) S_1' with SC_2 and D by XOR4LBs and stacking (h) S_1' with SC_1 and SC_2 by XOR4LBs and stacking

(i) S_2' with SC_1 and SC_2 (j) SC_1' (k) S_1' with SC_1' and D by XOR4LBs and stacking (l) S_1' with SC_2 and D by XOR4LBs and stacking

(m) S_1' with SC_1' and SC_2 by XOR4LBs and stacking (n) S_2' with SC_1' and SC_2

Fig. 6. Results of the designed ISSCommonAuthen, where $k = 2$ and $n = 2$. (a) A binary authentication image S_1; (b) a grayscale secret image S_2; (c)−(d) two grayscale shares SC_1 and SC_2; (e) the binary authentication share D preserved by the dealer; (f) the decrypted binary authentication image S_1' with SC_1 and D by XOR4LBs and stacking; (g) the decrypted binary authentication image S_1' with SC_2 and D by XOR4LBs and stacking; (h) the decrypted binary authentication image S_1' with SC_1 and SC_2; (i) the decrypted grayscale secret image S_2' with SC_1 and SC_2; (j) a fake share SC_1'; (k) the decrypted binary authentication image S_1' with SC_1' and D by XOR4LBs and stacking; (l) the decrypted binary authentication image S_1' with SC_2 and D by XOR4LBs and stacking; (m) the decrypted binary authentication image S_1' with SC_1' and SC_2; (n) the decrypted grayscale secret image S_2' with SC_1' and SC_2.

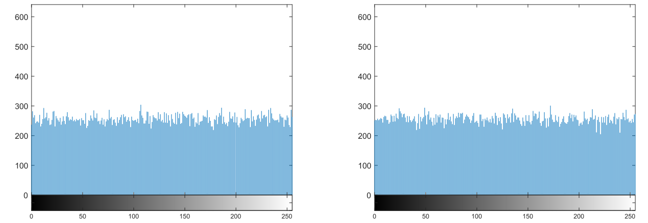

(a) Histogram of SC_1 (b) Histogram of SC_2

Fig. 7. Histograms of shares in Fig. 6.

authentication share D preserved by the dealer. Figs. 6 (f-h) show the decrypted binary authentication images S_1' with any two of SC_1, SC_2 and D by XOR4LBs and stacking, respectively, where the authentication image is well visually recognized, and thus, the corresponding share is authenticated. Fig. 6 (i) shows the grayscale secret image decrypted with the 2 shares based on Lagrange interpolation, where the secret image is losslessly decrypted, i.e., Fig. 6 (i) is the same as the adopted secret image in Fig. 6 (b). A randomly generated fake share, SC_1', is demonstrated in Fig. 6 (j), where each grayscale pixel value of the fake share is randomly generated. The decrypted binary authentication images S_1' with any two of SC_1', SC_2 and D by XOR4LBs and stacking, respectively, are indicated in Figs. 6 (k-m), where the authentication image is not visually decrypted, and thus, the share SC_1' is fake. Fig. 6 (n) demonstrates the grayscale secret image decrypted with SC_1' and SC_2 by Lagrange interpolation, which reveals nothing of the secret image; thus, the decryption has failed.

We note that the authentication is achieved by using VSS implemented based on probability theory. A binary authentication image with contrast loss may be viewed by stacking and human eyes to some degree in the case of fake or lossy share of a certain ratio. What is the range of tamper tolerant ratio for authentication application is decided by the just recognition point (JRD) of the clarity with regard to contrast in VSS [41]. When average tamper tolerant ratio for authentication application is larger than 0.4, it is hard to recognize the secret image.

In addition, Fig. 7 demonstrates share histograms of Figs. 6 (c-d). For each share, the pixel values are uniformly distributed in the range of $[0, 255]$, which to some extent, indicates each share decrypts nothing of the secret image and the security of the designed scheme.

In the following, we only illustrate the first share and the decrypted secret image with the first t shares to save space.

Fig. 8 displays the results of the designed ISSCommonAuthen, where $k = 3, n = 3$, the authentication image S_1 is demonstrated in Fig. 8 (a) and the grayscale secret image S_2 is presented in Fig. 8 (b). Fig. 8 (c) indicates the first share SC_1 of the output 3 shares. Fig. 8 (d) shows the output binary authentication share D. Figs. 8 (e-f) show the decrypted binary authentication images S_1' with SC_1 and D or SC_2 by XOR4LBs and stacking, respectively, where the authentication image is well visually recognized, and thus, the corresponding share is authenticated. Figs. 8 (g-h) show the grayscale secret images decrypted with the first 2 or more shares by Lagrange interpolation. From Figs. 8 (g-h), the secret image decrypted with all 3 shares is losslessly decrypted, while nothing of the secret image decrypted with 2 shares is recognized. A generated randomly fake share, SC_1', is demonstrated in Fig. 8 (i). The decrypted binary authentication images S_1' with SC_1' and D or SC_2 by XOR4LBs and stacking, respectively, are indicated in Figs. 8 (j-k), where the authentication image is not visually decrypted, and thus, the share SC_1' is fake. Figs. 8 (l-m) demonstrate the decrypted secret images S_2' with SC_1' and some other shares by Lagrange interpolation, which yields no clue about the original secret image; thus, the decryption has failed.

Fig. 9 displays the results of the designed ISSCommonAuthen, where $k = 3, n = 4$, the input binary authentication image S_1 is demonstrated in Fig. 9 (a) and the input grayscale secret image S_2 is displayed in Fig. 9 (b). Figs. 9 (c) indicates the first share SC_1 of the output 4 shares. Figs. 9 (d) shows the

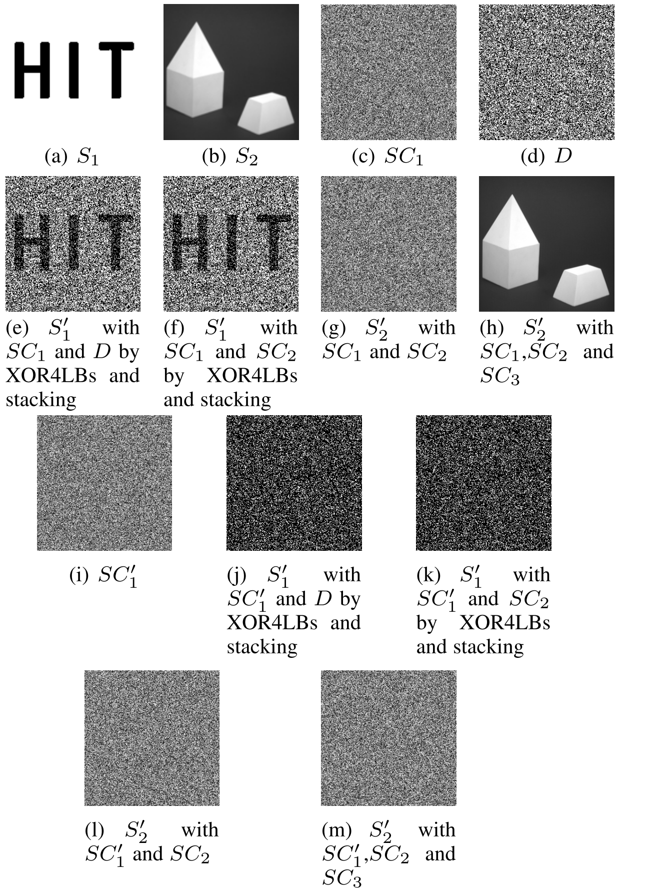

(a) S_1 (b) S_2 (c) SC_1 (d) D

(e) S_1' with SC_1 and D by XOR4LBs and stacking (f) S_1' with SC_1 and SC_2 by XOR4LBs and stacking (g) S_2' with SC_1 and SC_2 (h) S_2' with SC_1,SC_2 and SC_3

(i) SC_1' (j) S_1' with SC_1' and D by XOR4LBs and stacking (k) S_1' with SC_1' and SC_2 by XOR4LBs and stacking

(l) S_2' with SC_1' and SC_2 (m) S_2' with SC_1',SC_2 and SC_3

Fig. 8. Experimental results of the designed ISSCommonAuthen, where $k = 3$ and $n = 3$. (a) A binary authentication image S_1; (b) a grayscale secret image S_2; (c) grayscale share SC_1; (d) the binary authentication share D; (e) the decrypted binary authentication image S_1' with SC_1 and D by XOR4LBs and stacking; (f) the decrypted binary authentication image S_1' with SC_1 and D by XOR4LBs and stacking; (g)− (h) decrypted grayscale secret image S_2' with the first two or more shares; (i) a fake share SC_1'; (j) the decrypted binary authentication image S_1' with SC_1' and D by XOR4LBs and stacking; (k) the decrypted binary authentication image S_1' with SC_1' and D by XOR4LBs and stacking; (l)− (m) decrypted grayscale secret images S_2' with SC_1' and other one or more shares.

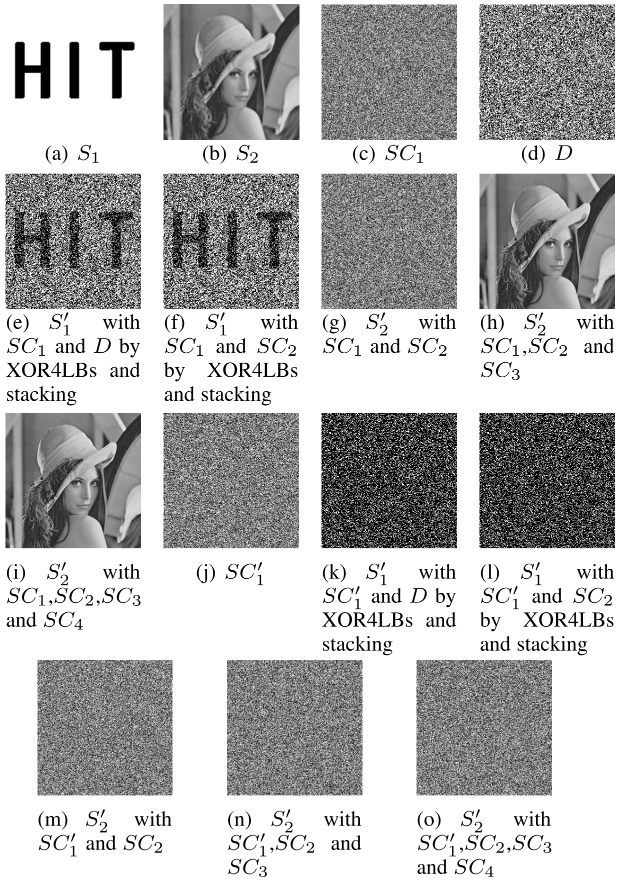

(a) S_1 (b) S_2 (c) SC_1 (d) D

(e) S_1' with SC_1 and D by XOR4LBs and stacking (f) S_1' with SC_1 and SC_2 by XOR4LBs and stacking (g) S_2' with SC_1 and SC_2 (h) S_2' with SC_1,SC_2 and SC_3

(i) S_2' with SC_1,SC_2,SC_3 and SC_4 (j) SC_1' (k) S_1' with SC_1' and D by XOR4LBs and stacking (l) S_1' with SC_1' and SC_2 by XOR4LBs and stacking

(m) S_2' with SC_1' and SC_2 (n) S_2' with SC_1',SC_2 and SC_3 (o) S_2' with SC_1',SC_2,SC_3 and SC_4

Fig. 9. Additional experimental results of the designed ISSCommonAuthen, where $k = 3$ and $n = 4$. (a) A binary authentication image S_1; (b) a grayscale secret image S_2; (c) the grayscale share SC_1; (d) the binary authentication share D; (e) the decrypted binary authentication image S_1' with SC_1 and D by XOR4LBs and stacking; (f) the decrypted binary authentication image S_1' with SC_1 and SC_2 by XOR4LBs and stacking; (g)− (i) the decrypted grayscale secret image S_2' with the first two or more shares; (j) a fake share SC_1'; (k) the decrypted binary authentication image S_1' with SC_1' and D by XOR4LBs and stacking; (l) the decrypted binary authentication image S_1' with SC_1' and SC_2 by XOR4LBs and stacking; (m)− (o) the decrypted grayscale secret images S_2' with SC_1' and other one or more shares.

output binary authentication share D. Figs. 9 (e-f) show the decrypted binary authentication images S_1' with SC_1 and D or SC_2 by XOR4LBs and stacking, respectively, where the authentication image is well visually recognized, and thus, the corresponding share is authenticated. Fig. 9 (g-i) shows the secret images decrypted with the first 2 or more shares by Lagrange interpolation. From Figs. 9 (g-i), the secret image decrypted with any 3 or more shares is losslessly decrypted, while nothing of the secret image decrypted with 2 or fewer shares is recognized. A generated randomly fake share, SC_1', is demonstrated in Fig. 9 (j). The decrypted binary authentication images S_1' with SC_1' and D or SC_2 by XOR4LBs and stacking, respectively, are indicated in Figs. 9 (k-l), where the authentication image is not visually decrypted and thus, the share SC_1' is fake. Figs. 9 (m-o) demonstrate the decrypted secret images S_2' with SC_1' and other one or more first shares by Lagrange interpolation, which yield no clue about the secret image; thus, the decryption is failed.

From the above experiments, we can conclude the following.

1) Each share has no pixel expansion and no cross-interference of the secret image.
2) With fewer than k shares no secret is leaked, which shows the security of the designed ISS.
3) The secret image is losslessly decrypted with any k or more shares.
4) Without sending the share itself, the separate share is visually decrypted to achieve authentication by only XORing and stacking operations, which are only simple operations with low computational complexity.
5) The authentication abilities of both dealer participatory authentication and dealer nonparticipatory authentication are achieved through fusing VSS and polynomial-based ISS.
6) An ISS with separate common share authentication ability for a general (k, n)-threshold is achieved, where $n \geq k \geq 2$.

We note the following.

1) As examples, Fig. 6, Fig. 8 and Fig. 9 are used to validate the effectiveness (characteristics or features)

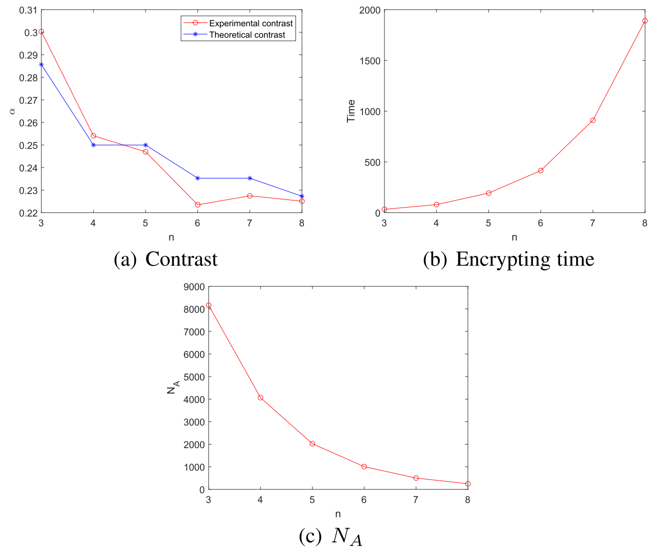

(a) Contrast

(b) Encrypting time

(c) N_A

Fig. 10. Contrast, encrypting time and N_A curves for n when $x = 4, k = 3$.

of the designed scheme, where typical thresholds and images are tested.

2) The secret image can be losslessly decrypted by Lagrange interpolation with any k or more shares; thus, any grayscale secret can be input in the designed scheme.

3) Because Definition 1 is given by a statistical result, in VSS the experimental results will be close to the theoretical contrast. Therefore, any binary authentication image can be input in the designed scheme, where close contrast of the decrypted binary authentication image will be obtained. Moreover, the contrast will to some degree determine how well human eyes may recognize the decrypted binary authentication image. For clarity corresponding to different contrast values, please refer to [41].

4) As a result, we only give some typical experimental results.

B. Available Parameters and Quality Discussions

We will study the parameters of contrast, encrypting time and N_A for k and n given that k and n play important roles in the scheme, where the contrast is that of the decrypted binary authentication image S'_1 with SC_1 and SC_2 by XOR4LBs and stacking. Here, x means the x low bits of the share are XORed, where in our designed scheme $x = 4$. We also intend to study our rationale for setting $x = 4$. The authentication image and grayscale secret image with a size of 128×128 in Fig. 6 are employed in our experiments.

Fig. 10 shows the contrast, encrypting time and N_A curves for n when $k = 3$, where the theoretical contrast is given as well, from which we know the following:

1) The contrast is an approximately monotonically decreasing function of n. The experimental contrast fits with the theoretical analysis, which shows the effectiveness of our analyses.

2) The encrypting time is a monotonically dramatically increasing function of n. As n increases, the screening conditions increase, and thus, the encrypting time increases.

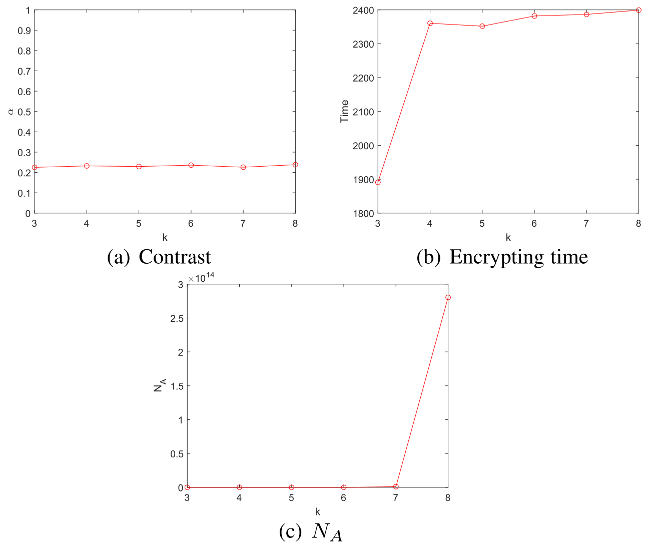

(a) Contrast

(b) Encrypting time

(c) N_A

Fig. 11. Contrast, encrypting time and N_A curves for k when $x = 4, n = 8$.

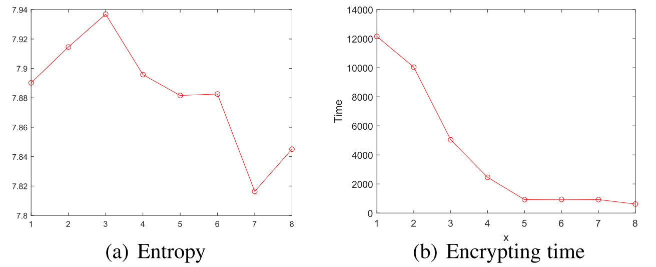

(a) Entropy

(b) Encrypting time

Fig. 12. Entropy, and encrypting time curves for x when $k = 2, n = 6$, $N_A = 16$.

3) N_A is a monotonically decreasing function of n. As n increases, the screening conditions increase, and thus, the number of random values decreases.

Fig. 11 shows the contrast, encrypting time and N_A curves for k when $n = 8$, from which we know the following:

1) The contrast is nearly the same as k increases. Because $S_1C_1, S_1C_2, \cdots S_1C_{n+1}$ construct a $(2, n+1)$-threshold VSS without relations with k.

2) The encrypting time is a monotonically dramatically increasing function of k and slightly increasing when $k \geq 4$. As k increases, the screening space increases, and when $k \geq 4$, the alternative random values increases.

3) N_A is a monotonically increasing function of k and dramatically increasing when $k \geq 7$. As k increases, the number of random values dramatically increases.

Fig. 12 intends to convey the rationale for setting $x = 4$ as follows, where $k = 2, n = 6, N_A = 16$, the entropy is computed by Eq. (8), and the result is that of SC_1.

$$H(Y) = -\sum_{y \in Y} Prob(y) \log_2 Prob(y) \tag{8}$$

1) In our algorithm, $H \geq 7.88$ is suggested in order to achieve acceptable security, which is obtained from extensive experiments.

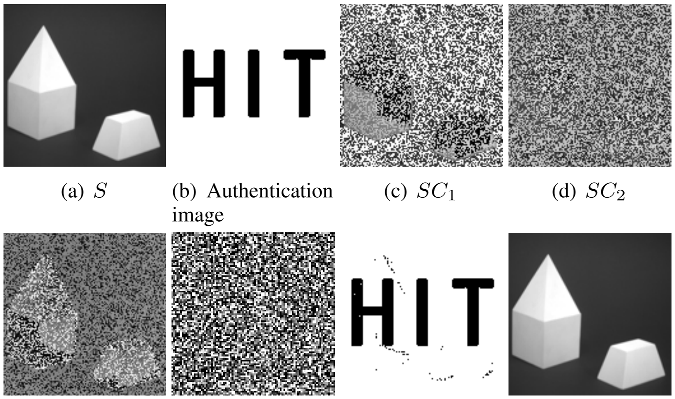

(a) S

(b) Authentication image

(c) SC_1

(d) SC_2

(e) SC_3

(f) Additional image

(g) Authentication result of SC_1 by the dealer

(h) S' decrypted with SC_1 and SC_2

Fig. 13. Experiments of Yan *et al.*, where $k = 2$ and $n = 3$. (a) A grayscale secret image S; (b) a binary authentication image; (c)− (e) shares SC_1, SC_2 and SC_3; (f) additional binary image preserved by the dealer; (g) the authentication result of SC_1 by the dealer; (f) grayscale secret image S' with SC_1 and SC_2.

2) 1, 2, 3 and 4 are alternative values of x given that their entropies are larger than 7.88.
3) Considering the encrypting time, $x = 4$ consumes an acceptable time.
4) In our algorithm, we set $x = 4$ to balance the security and the encrypting time.

C. Comparisons With Related Schemes

We will compare the designed ISSCommonAuthen with the related schemes in terms of illustrations and/or features.

First, we will compare our method with that of Yan *et al*. [36] by means of experiments and features where the same secret image as Fig. 13(a) and the $(2, 3)$ threshold will be used. The scheme of Yan *et al* is chosen for comparison because their scheme has a separate shadow authentication ability for a (k, n) threshold that is also based on a polynomial.

Fig. 13 is the experiment of Yan *et al.*, where $k = 2$ and $n = 3$, and a grayscale secret image S is in Fig. 13 (a). Fig. 13 (b) is a binary authentication image. Figs. 13 (c-e) shows the three output shares SC_1, SC_2 and SC_3. Fig. 13 (f) displays the binary image preserved by the dealer for authentication. Fig. 13 (g) shows the authentication result of SC_1 by the dealer. Fig. 13 (h) shows the secret image decrypted by Lagrange interpolation with the first 2 shadow images. From Fig. 13 (h), the decrypted secret image with any 2 or more shares is lossless.

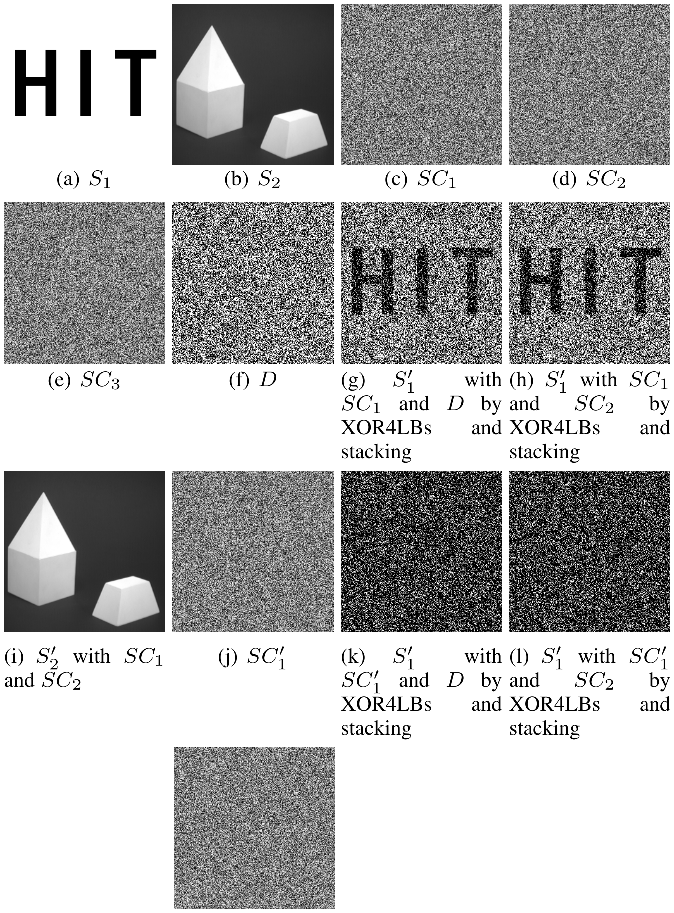

(a) S_1

(b) S_2

(c) SC_1

(d) SC_2

(e) SC_3

(f) D

(g) S_1' with SC_1 and D by XOR4LBs and stacking

(h) S_1' with SC_1 and SC_2 by XOR4LBs and stacking

(i) S_2' with SC_1 and SC_2

(j) SC_1'

(k) S_1' with SC_1' and D by XOR4LBs and stacking

(l) S_1' with SC_1' and SC_2 by XOR4LBs and stacking

(m) S_2' with SC_1' and SC_2

Fig. 14. Experimental results of the designed ISSCommonAuthen, where $k = 2$ and $n = 3$. (a) A binary authentication image S_1; (b) a grayscale secret image S_2; (c-e) grayscale shares SC_1, SC_2 and SC_3; (f) the binary authentication share D; (g) the decrypted binary authentication image S_1' with SC_1 and D by XOR4LBs and stacking; (h) the decrypted binary authentication image S_1' with SC_1 and D by XOR4LBs and stacking; (i) decrypted grayscale secret image S_2' with the first two shares; (j) a fake share SC_1'; (k) the decrypted binary authentication image S_1' with SC_1' and D by XOR4LBs and stacking; (l) the decrypted binary authentication image S_1' with SC_1' and SC_2 by XOR4LBs and stacking; (m) decrypted grayscale secret images S_2' with SC_1' and the other one share.

Fig. 14 displays the results of the designed ISSCommonAuthen with the same parameters, where $k = 2, n = 3$, the input binary authentication image S_1 is demonstrated in Fig. 14 (a) and the input grayscale secret image S_2 is displayed in Fig. 14 (b). Fig. 14 (c-e) indicate the three shares SC_1, SC_2 and SC_3. Fig. 14 (f) shows the output binary authentication share D. Figs. 14 (g-h) show the decrypted binary authentication images S_1' with SC_1 and D or SC_2 by XOR4LBs and stacking, respectively, where the authentication image is well visually recognized, and thus, the corresponding share is authenticated. Figs. 14 (i) shows the grayscale secret images decrypted with the first 2 shares by Lagrange interpolation. From Fig. 14 (i), the secret image decrypted with any 2 or more shares is losslessly decrypted. A generated randomly fake share, SC_1', is demonstrated in Fig. 14 (j). The decrypted binary authentication images S_1' with SC_1' and D or SC_2 by XOR4LBs and stacking, respectively, are indicated in Figs. 14 (k-l), where the authentication image is not visually decrypted, and thus, the share SC_1' is fake. Fig. 14 (m) demonstrates the decrypted secret images S_2' with SC_1' and SC_2 by Lagrange interpolation, which yields no clue about the secret image; thus, the decryption has failed.

According to Figs. 13 and 14, the two schemes are compared as follows.

1) Both schemes have the features of dealer participatory separate shadow image authentication ability, no pixel

TABLE I

TIME COMPLEXITY COMPARISON WITH THE RELATED SCHEMES OF LIU *et al.* [35] AND LIU AND CHANG [31]

Scheme	Threshold	Decryption operation	Decryption complexity	Authentication operation	Authentication complexity
Liu *et al.*	(k, n)	Interpolation	$O(k \log^2 k)$	Interpolation	$O(k \log^2 k)$
Liu and Chang	$(2, 2)$	Matrix turtle shell (MTS), lookup, judge, etc.	Hard to evaluate	MTS, lookup, compare, etc.	Hard to evaluate
Ours	(k, n)	Interpolation	$O(k \log^2 k)$	XOR and OR	$O(k)$

expansion, lossless decoding, the (k, n) threshold and use of a polynomial.

2) The scheme of Yan *et al*. can authenticate the shadow image only by the dealer, i.e., dealer participatory authentication, while our method has authentication abilities of both dealer participatory authentication and dealer nonparticipatory authentication.

3) The scheme of Yan *et al* may have slight information leakage in the shadow image since they only utilize the most significant bit in their scheme; however, because we set $x = 4$ to balance the security and the efficiency, there is no information leakage in our method.

4) Only the binarization operation is needed for authentication in the scheme of Yan *et al*., which is slightly lower than ours.

Second, we will compare the designed ISSCommonAuthen with Jiang *et al.*'s work [37]. Actually, Jiang *et al.*'s work is a special case of our scheme when $x = 1$. According to Fig. 12, Jiang *et al.*'s scheme needs larger encrypting time than ours. More importantly, because using LSB leads to a smaller value of N_A than using $4LBs$ when value of $n - k$ is larger, their scheme may have failed authentication with a larger value of $n - k$, and the number of brute-force attacks will be reduced.

Third, we will compare the designed ISSCommonAuthen with the related schemes of Liu *et al.* [35] and Liu and Chang [31] by means of qualitative analyses and time complexity. These schemes are chosen to compare because they also have share authentication ability of ISS. Only qualitative analyses are given rather than a quantitative comparison and illustration because the features are significantly different between theirs and ours, and in addition, only a theoretical proof is performed in Liu *et al.* [35].

1) In Liu and Chang's scheme, the share authentication ability is chiefly realized based on a turtle shell-based information hiding, among which each share is embedded into a cover image by using information hiding technique. However, it leads to a pixel expansion and high decryption (authentication) complexity. More importantly, their scheme is only suitable for dealer participatory authentication with share sending. By contrast, the designed scheme is suitable for both dealer participatory authentication and dealer nonparticipatory authentication without share sending, which is achieved based on ISS itself rather than information hiding. The authentication is performed based on only XORing and stacking; thus, the designed scheme has low decryption (authentication) complexity and no pixel expansion. Their scheme can achieve tamper detection and location, while ours cannot.

2) Liu *et al.* embeds an authentication value into a coefficient of the polynomial to extend follow-up improved polynomial-based ISS to achieve share authentication in the field of 251. It can only find the existence of a fake participant when collecting any k or more shares; however, it cannot distinguish which one is fake. Thus, it suffers from lossy decryption, auxiliary encryption, hard fake participant location, and high decryption (authentication) complexity. More importantly, their scheme is only suitable for dealer participatory authentication with share sending. By contrast, the designed scheme is suitable for both dealer participatory authentication and dealer nonparticipatory authentication without share sending. Our scheme can detect each share when collecting the share to achieve separate share authentication ability in the field of 257 with lossless decryption, low encryption and decryption (authentication) complexity, and no auxiliary encryption.

3) Table I shows the theoretical comparison for the time complexity in the stages of the decryption and authentication. Both Liu *et al.*'s scheme and ours are for the (k, n) threshold, while Liu and Chang's scheme is for the $(2, 2)$ threshold. Since there are many operations in Liu and Chang's scheme and the time complexity analysis is not given in their paper, it is hard for us to evaluate the time complexity. Compared with Liu *et al.*'s scheme, our scheme has the same decryption complexity and lower authentication complexity. In a word, our scheme has admirable decryption and authentication time complexity compared with related schemes.

In summary, compared with the abovementioned schemes, the designed ISSCommonAuthen has the following advantages.

1) Our method is suitable for both dealer participatory authentication and dealer nonparticipatory authentication.
2) The designed ISSCommonAuthen achieves separate share authentication, which can authenticate the share when receiving any other one share.
3) The output share has no pixel expansion, which will save storage.
4) The operation of authentication is simple and no auxiliary encryption is needed, which will save computational power.
5) The secret image are losslessly decrypted.

V. CONCLUSION

In this paper, we have designed an ISS for a (k, n)-threshold with a separate common share authentication ability, which are suitable for both dealer participatory authentication and dealer nonparticipatory authentication. The designed ISS fuses the principles of polynomial and VSS to achieve the additional features of separate share authentication, no pixel expansion, low encryption and decryption (authentication) complexity, lossless decryption and auxiliary encryption. The experimental illustrations and theoretical analyses have shown the effectiveness of the designed scheme. We have performed feature comparisons with the related schemes to present the advantages of our scheme. We chiefly focus on the following works in the future. First, we will extend our scheme to achieve tamper detection and location. Second, we will apply some other typical ISS principles to our scheme, such as the Chinese remainder theorem-based ISS. Third, we will study the tamper tolerant ratio.

Acknowledgment

The authors would like to thank the anonymous reviewers for their valuable comments.

References

[1] A. A. A. El-Latif, B. Abd-El-Atty, W. Mazurczyk, C. Fung, and S. E. Venegas-Andraca, "Secure data encryption based on quantum walks for 5G Internet of Things scenario," *IEEE Trans. Netw. Service Manage.*, vol. 17, no. 1, pp. 118–131, Mar. 2020.

[2] Y. Zhang, C. Qin, W. Zhang, F. Liu, and X. Luo, "On the fault-tolerant performance for a class of robust image steganography," *Signal Process.*, vol. 146, pp. 99–111, May 2018. [Online]. Available: http://www.sciencedirect.com/science/article/pii/S016516841830001X

[3] X. Zhang, F. Peng, and M. Long, "Robust coverless image steganography based on DCT and LDA topic classification," *IEEE Trans. Multimedia*, vol. 20, no. 12, pp. 3223–3238, Dec. 2018.

[4] L. Li, M. S. Hossain, A. A. A. El-Latif, and M. F. Alhamid, "Distortion less secret image sharing scheme for Internet of Things system," *Cluster Comput.*, vol. 22, no. 1, pp. 2293–2307, Nov. 2017, doi: 10.1007/s10586-017-1345-y.

[5] M. Fukumitsu, S. Hasegawa, J. Iwazaki, M. Sakai, and D. Takahashi, "A proposal of a secure p2p-type storage scheme by using the secret sharing and the blockchain," in *Proc. IEEE 31st Int. Conf. Adv. Inf. Netw. Appl. (AINA)*, Mar. 2017, pp. 803–810.

[6] Y. Cheng, Z. Fu, and B. Yu, "Improved visual secret sharing scheme for QR code applications," *IEEE Trans. Inf. Forensics Security*, vol. 13, no. 9, pp. 2393–2403, Sep. 2018.

[7] A. A. A. El-Latif, B. Abd-El-Atty, M. S. Hossain, M. A. Rahman, A. Alamri, and B. B. Gupta, "Efficient quantum information hiding for remote medical image sharing," *IEEE Access*, vol. 6, pp. 21075–21083, 2018.

[8] P. Wang, X. He, Y. Zhang, W. Wen, and M. Li, "A robust and secure image sharing scheme with personal identity information embedded," *Comput. Secur.*, vol. 85, pp. 107–121, Aug. 2019.

[9] P. V. Chavan, M. Atique, and L. Malik, "Signature based authentication using contrast enhanced hierarchical visual cryptography," in *Proc. Electr., Electron. Comput. Sci.*, 2014, pp. 1–5.

[10] Y. Li and L. Guo, "Robust image fingerprinting via distortion-resistant sparse coding," *IEEE Signal Process. Lett.*, vol. 25, no. 1, pp. 140–144, Jan. 2018.

[11] S. Zou, Y. Liang, L. Lai, and S. Shamai, "An information theoretic approach to secret sharing," 2014, *arXiv:1404.6474*. [Online]. Available: http://arxiv.org/abs/1404.6474

[12] I. Komargodski, M. Naor, and E. Yogev, "Secret-sharing for NP," *J. Cryptol.*, vol. 30, no. 2, pp. 444–469, Apr. 2017.

[13] G. Wang, F. Liu, and W. Q. Yan, "Basic visual cryptography using braille," *Int. J. Digit. Crime Forensics*, vol. 8, no. 3, pp. 85–93, Jul. 2016.

[14] M. Naor and A. Shamir, "Visual cryptography," in *Cryptology-EUROCRYPT* (Lecture Notes in Computer Science). Perugia, Italy: Springer, 1995, pp. 1–12.

[15] C.-N. Yang, C.-C. Wu, and Y.-C. Lin, "*k* out of *n* region-based progressive visual cryptography," *IEEE Trans. Circuits Syst. Video Technol.*, vol. 29, no. 1, pp. 252–262, Jan. 2019.

[16] A. Shamir, "How to share a secret," *Commun. ACM*, vol. 22, no. 11, pp. 612–613, Nov. 1979.

[17] X. Yan, L. Liu, L. Li, and Y. Lu, "Robust secret image sharing resistant to noise in shares," *ACM Trans. Multimedia Comput., Commun., Appl.*, Oct. 2020.

[18] C. Asmuth and J. Bloom, "A modular approach to key safeguarding," *IEEE Trans. Inf. Theory*, vol. IT-29, no. 2, pp. 208–210, Mar. 1983.

[19] X. Yan, Y. Lu, L. Liu, and X. Song, "Reversible image secret sharing," *IEEE Trans. Inf. Forensics Security*, vol. 15, no. 5, pp. 3848–3858, Oct. 2020.

[20] Z. Wang, G. R. Arce, and G. Di Crescenzo, "Halftone visual cryptography via error diffusion," *IEEE Trans. Inf. Forensics Security*, vol. 4, no. 3, pp. 383–396, Sep. 2009.

[21] J. Weir and W. Yan, *A comprehensive study of visual cryptography*, vol. 5. Berlin, Germany: Springer, 2010, pp. 70–105.

[22] X. Yan, S. Wang, X. Niu, and C.-N. Yang, "Halftone visual cryptography with minimum auxiliary black pixels and uniform image quality," *Digit. Signal Process.*, vol. 38, pp. 53–65, Mar. 2015.

[23] Z.-X. Fu and B. Yu, "Visual cryptography and random grids schemes," in *Digital-Forensics Watermarking*. Auckland, New Zealand: Springer, 2014, pp. 109–122.

[24] X. Yan, X. Liu, and C.-N. Yang, "An enhanced threshold visual secret sharing based on random grids," *J. Real-Time Image Process.*, vol. 14, no. 1, pp. 61–73, Jan. 2018.

[25] T. Guo, F. Liu, and C. Wu, "Threshold visual secret sharing by random grids with improved contrast," *J. Syst. Softw.*, vol. 86, no. 8, pp. 2094–2109, Aug. 2013.

[26] C.-C. Thien and J.-C. Lin, "Secret image sharing," *Comput. Graph.*, vol. 26, no. 5, pp. 765–770, Oct. 2002.

[27] Y. Liu, C. Yang, Y. Wang, L. Zhu, and W. Ji, "Cheating identifiable secret sharing scheme using symmetric bivariate polynomial," *Inf. Sci.*, vol. 453, pp. 21–29, Jul. 2018.

[28] X. Zhou, Y. Lu, X. Yan, Y. Wang, and L. Liu, "Lossless and efficient polynomial-based secret image sharing with reduced shadow size," *Symmetry*, vol. 10, no. 7, 2018. [Online]. Available: http://www.mdpi.com/2073-8994/10/7/249

[29] Z. Zhou, C. Yang, Y. Cao, and X. Sun, "Secret image sharing based on encrypted pixels," *IEEE Access*, vol. 6, p. 15021–15025, 2018.

[30] C.-C. Lin and W.-H. Tsai, "Secret image sharing with steganography and authentication," *J. Syst. Softw.*, vol. 73, no. 3, pp. 405–414, Nov. 2004.

[31] Y. Liu and C.-C. Chang, "A turtle shell-based visual secret sharing scheme with reversibility and authentication," *Multimedia Tools Appl.*, vol. 77, no. 19, pp. 25295–25310, Oct. 2018, doi: 10.1007/s11042-018-5785-z.

[32] C.-C. Chang, Y.-P. Hsieh, and C.-H. Lin, "Sharing secrets in stego images with authentication," *Pattern Recognit.*, vol. 41, no. 10, pp. 3130–3137, Oct. 2008. [Online]. Available: http://www.sciencedirect.com/science/article/pii/S0031320308001374

[33] G. Ulutas, M. Ulutas, and V. V. Nabiyev, "Secret image sharing scheme with adaptive authentication strength," *Pattern Recognit. Lett.*, vol. 34, no. 3, pp. 283–291, Feb. 2013. [Online]. Available: http://www.sciencedirect.com/science/article/pii/S0167865512003479

[34] P. Li, P. Ma, and X. Su, "Image secret sharing and hiding with authentication," in *Proc. 1st Int. Conf. Pervas. Comput., Signal Process. Appl.*, Sep. 2010, pp. 367–370.

[35] Y.-X. Liu, Q.-D. Sun, and C.-N. Yang, "(k,n) secret image sharing scheme capable of cheating detection," *EURASIP J. Wireless Commun. Netw.*, vol. 2018, no. 1, p. 72, Apr. 2018, doi: 10.1186/s13638-018-1084-7.

[36] X. Yan, Q. Gong, L. Li, G. Yang, Y. Lu, and J. Liu, "Secret image sharing with separate shadow authentication ability," *Signal Process., Image Commun.*, vol. 82, Mar. 2020, Art. no. 115721. [Online]. Available: http://www.sciencedirect.com/science/article/pii/S0923596519306940

[37] Y. Jiang, X. Yan, J. Qi, Y. Lu, and X. Zhou, "Secret image sharing with dealer-participatory and Non-Dealer-Participatory mutual shadow authentication capabilities," *Mathematics*, vol. 8, no. 2, p. 234, Feb. 2020.

[38] R. De Prisco and A. De Santis, "On the relation of random grid and deterministic visual cryptography," *IEEE Trans. Inf. Forensics Security*, vol. 9, no. 4, pp. 653–665, Apr. 2014.

[39] C.-N. Yang, C.-C. Wu, and D.-S. Wang, "A discussion on the relationship between probabilistic visual cryptography and random grid," *Inf. Sci.*, vol. 278, pp. 141–173, Sep. 2014.

[40] O. Kafri and E. Keren, "Encryption of pictures and shapes by random grids," *Opt. Lett.*, vol. 12, no. 6, pp. 377–379, 1987.

[41] X. Yan, Y. Lu, H. Huang, L. Liu, and S. Wan, "Clarity corresponding to contrast in visual cryptography," in *Proc. 2nd Int. Conf. Young Comput. Sci., Eng.*, Harbin, China, Aug. 2016, pp. 249–257, 2016, doi: 10.1007/978-981-10-2053-7_23.

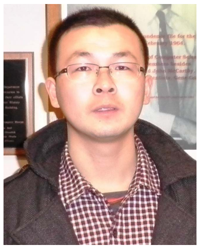

Xuehu Yan was born in China, in February 1984. He received the B.Sc. degree (Hons.) in science in information and calculate science, the M.Sc. degree in computational mathematics, and the Ph.D. degree in computer science and technology from the Harbin Institute of Technology, China, in 2006, 2008, and 2015, respectively. He is currently an Associate Professor with the National University of Defense Technology, Hefei, China. His areas of interests are visual cryptography, secret image sharing information hiding, cryptography, and multimedia security He has published more than 100 articles in these areas. He is an Associate Editor of the *International Journal of Digital Crime and Forensics* (IJDCF).

Yuliang Lu was born in China, in 1964. He received the B.Sc. degree (Hons.) in computer application and the M.Sc. degree in computer application from Southeast University, China, in 1985 and 1988, respectively. He is currently a Professor with the National University of Defense Technology, Hefei, China. His area of interests are computer applications and information processing.

Ching-Nung Yang (Senior Member, IEEE) received the B.S. and M.S. degrees in telecommunication engineering from National Chiao Tung University, Hsinchu, Taiwan, in 1983 and 1985, respectively, and the Ph.D. degree in electrical engineering from National Cheng Kung University, Tainan City, Taiwan, in 1997. He is currently a Full Professor with the Department of Computer Science and Information Engineering, National Dong Hwa University, Hualien, Taiwan. His research interests include coding theory, information security, and cryptography. He is a fellow of IET.

Xinpeng Zhang received the B.S. degree in computational mathematics from Jilin University, China, in 1995, and the M.E. and Ph.D. degrees in communication and information system from Shanghai University, China, in 2001 and 2004, respectively. Since 2004, he was with the faculty of the School of Communication and Information Engineering, Shanghai University, where he is currently a Professor. He was with The State University of New York at Binghamton as a Visiting Scholar from 2010 to 2011, and also with Konstanz University as an experienced Researcher, sponsored by the Alexander von Humboldt Foundation from 2011 to 2012. He is also with the faculty of the School of Computer Science, Fudan University. His research interests include multimedia security, image processing, and digital forensics. He has published more than 200 papers in these areas. He was an Associate Editor of the IEEE TRANSACTIONS ON INFORMATION FORENSICS AND SECURITY from 2014 to 2017.

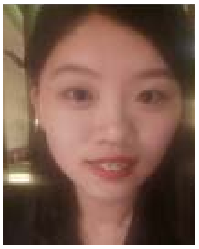

Shudong Wang was born in China, in 1997. She received the B.Sc. degree in network engineering from the National University of Defense Technology, Hefei, China, in 2019, where she is currently pursuing the master's degree. Her area of interests are computer security, multimedia security, and secret image sharing.